

Geophysical Research Letters

RESEARCH LETTER

10.1029/2018GL079121

Partitioning Evapotranspiration Over the Continental United States Using Weather Station Data

Angela J. Rigden¹ , Guido D. Salvucci² , Dara Entekhabi³ , and Daniel J. Short Gianotti³ 

¹Department of Earth and Planetary Sciences, Harvard University, Cambridge, MA, USA, ²Department of Earth and Environment, Boston University, Boston, MA, USA, ³Department of Civil and Environmental Engineering, MIT, Cambridge, MA, USA

Abstract Accurately characterizing evapotranspiration is critical when predicting the response of the hydrologic cycle to climate change. Although Earth system models estimate similar magnitudes of global evapotranspiration, the magnitude of each contributing source varies considerably between models due to the lack of evapotranspiration partitioning data. Here we develop an observation-based method to partition evapotranspiration into soil evaporation and transpiration using meteorological data and satellite soil moisture retrievals. We apply the methodology at 1,614 weather stations across the continental United States during the summers of 2015 and 2016. We evaluate the method using vegetation indices inferred from satellites, finding strong spatial correlations between modeled transpiration and solar-induced fluorescence ($r^2 = 0.87$), and modeled vegetation fraction and leaf area index ($r^2 = 0.70$). Since the sensitivity of evapotranspiration to environmental factors depends on the contribution of each source component, understanding the partitioning of evapotranspiration is increasingly important with climate change.

Plain Language Summary Water moves from the land surface to the overlying atmosphere by evaporation. The two main sources of evaporation include (1) evaporation from soils and (2) evaporation from pores on plants, called *transpiration*. Although methods exist to measure total evaporation over an ecosystem, it is challenging to observe soil evaporation and transpiration separately over an ecosystem. Consequently, the amount of estimated soil evaporation and transpiration varies considerably across models. In this study, we develop an observation-based method to estimate the fraction of water moved from the land to the atmosphere by plants, or the fraction of total evaporation that comes from transpiration. The method primarily relies on weather station data and soil moisture estimates from a recently launched satellite. We apply the method across the continental United States during the summers of 2015 and 2016 and evaluate it using observations of plants inferred from other satellites. Looking toward the future, it is important to estimate transpiration and soil evaporation correctly because they respond differently to changes in climate.

Citation:

Rigden, A. J., Salvucci, G. D., Entekhabi, D., & Short Gianotti, D. J. (2018). Partitioning evapotranspiration over the continental United States using weather station data. *Geophysical Research Letters*, 45, 9605–9613. <https://doi.org/10.1029/2018GL079121>

Received 8 JUN 2018
Accepted 25 AUG 2018
Accepted article online 31 AUG 2018
Published online 21 SEP 2018

1. Introduction

Evapotranspiration (ET) represents the total movement of water from the land surface to the atmosphere via transpiration, soil evaporation, and canopy evaporation. While modern Earth system models generally agree on the magnitude of total ET, the magnitude of each source component differs substantially between models (e.g., Kumar et al., 2018; Lawrence et al., 2007; Wei et al., 2017). For example, in the Coupled Model Intercomparison Project 5 simulations, the percent of global ET partitioned to transpiration (T/ET) varies from 22% to 58% (Wei et al., 2017). Across land surface models, isotope analyses, and remote sensing-based products, estimates of global T/ET span from approximately 25% to 85% (see Figure 4 in Wei et al., 2017). This large uncertainty in global T/ET is predominantly due to a lack of transpiration and soil evaporation observations at relevant spatial and temporal scales for model formulation, calibration, and validation.

At smaller scales, researchers have gained much insight into the controls of soil evaporation and transpiration by measuring and modeling each flux separately (Kool et al., 2014). Soil evaporation has been measured and modeled for decades (e.g., Black et al., 1969; Richards et al., 1956; Ritchie, 1972), and various parameterizations relating bare soil evaporation to soil moisture (SM) have been proposed (Mahfouf & Noilhan, 1991). Additionally, leaf level stomatal controls on transpiration have been extensively explored (see review by Damour et al., 2010), and the issues of scaling from leaf to region have been thoroughly discussed,

Clear main message in both the title and abstract



Putting main message into context immediately



Background:

Research gap:

particularly in regard to the micrometeorological feedbacks present at larger spatial scales (Jarvis & McNaughton, 1986; McNaughton & Jarvis, 1991; McNaughton & Spriggs, 1986). Generally, the underlying processes governing soil evaporation and transpiration at smaller scales are spatially upscaled to serve as the basis of ET models within Earth system models. This scaling requires numerous, soil- and vegetation-specific effective parameters, which, again, cannot be sufficiently calibrated and validated with direct observations when implemented in Earth system models.

Measurements from eddy covariance towers have been widely utilized to characterize ET partitioning at ecosystem scales. For example, to better constrain T/ET researchers have leveraged observations from multiple towers within and above the canopy (e.g., Baldocchi et al., 1997; Moore et al., 1996), compared ET and SM dynamics from coexisting sites with contrasting vegetation types (e.g., Baldocchi et al., 2004), coupled measurements of carbon and water fluxes (Scanlon & Kustas, 2010; Scanlon & Sahu, 2008; Scott & Biederman, 2017; Zhou et al., 2016), measured sap flow (e.g., Oishi et al., 2010; Wilson et al., 2001) or stable isotopes (e.g., Yopez et al., 2003) in conjunction with water fluxes, and quantified the degree to which the canopy is coupled to atmosphere with respect to seasonality (e.g., Wilson et al., 2000). Although analyses of eddy covariance measurements have revealed important phenomenon governing the transport of water from the land surface to the atmosphere, synthesizing these observations to inform Earth system models has largely been hampered by their mismatch in temporal scales, as processes governing soil evaporation and transpiration vary diurnally (Wang et al., 2010) and seasonally (Wang et al., 2014), and such studies have limited periods of record.

Clear research objective

In this study, we aim to develop an observation-based approach to partition ET into soil evaporation and transpiration that can be applied across large spatial scales. Rather than scaling the physical processes governing soil evaporation and transpiration (as common in land surface models), we build a statistical approach to decompose ET into its transpiration and soil evaporation components at common weather stations. In the statistical approach, we utilize meteorological observations from the weather stations, SM observations from the Soil Moisture Active Passive (SMAP) satellite (Entekhabi et al., 2010), and a recently developed method to estimate ET at each weather station, called the *Evapotranspiration from Relative Humidity at Equilibrium* (ETRHEQ) method (Rigden & Salvucci, 2015, 2017; Salvucci & Gentine, 2013).

2. Methods

2.1. Estimating ET With ETRHEQ Method

Daily ET is estimated using the ETRHEQ method (Rigden & Salvucci, 2015, 2017; Salvucci & Gentine, 2013). The ETRHEQ method is structured as “big-leaf” model and uses a daily effective surface conductance to water vapor transport (C_{surf}) to estimate ET. Unlike land surface models, which estimate conductances and ET via surface parameterizations, the ETRHEQ method utilizes an emergent relation between the land surface and the diurnal cycle of relative humidity to determine daily C_{surf} and thus ET. These C_{surf} estimates serve as the foundation of this study, as they enable us to estimate transpiration and soil evaporation without needing to prescribe surface parameterizations (as described in section 2.3).

To estimate C_{surf} , the ETRHEQ method requires hourly meteorological data collected at weather stations including temperature, humidity, wind speed, and pressure, as well as solar radiation. The only surface parameters required by the ETRHEQ method are an estimate of vegetation height to characterize roughness lengths (Rigden & Salvucci, 2017), an estimate of emissivity (assumed constant at 0.98), and a single estimate of soil thermal inertia to calculate ground heat flux (calibrated with eddy covariance data, $1,300 \text{ Jm}^{-2} \text{ s}^{-1/2} \text{ K}^{-1}$; Rigden & Salvucci, 2017). No additional knowledge of the surface is required; thus, inputs do not include estimates of SM, leaf area index (LAI), or vegetation fraction. The ETRHEQ method agrees well with measurements at over 60 eddy covariance sites—spanning a diverse range of plant functional types and climates (Rigden & Salvucci, 2017)—and watershed-scale estimates of ET across the continental United States (Rigden & Salvucci, 2015). Since the ETRHEQ method has primarily been evaluated with respect to surface fluxes, we directly evaluate the ETRHEQ method's ability to estimate daily C_{surf} inferred from eddy covariance data (following similar methods as Rigden & Li, 2017) at 48 towers across the United States (Table S1 in the supporting information), finding good performance across sites (Figure S1). For clarity, we refer to the C_{surf} estimates from the ETRHEQ method as “ $C_{surf, EQ}$ ”.

2.2. Data

2.2.1. ETRHEQ Inputs

Hourly temperature, humidity, wind speed, and pressure are from the National Oceanic and Atmospheric Administration's National Climatic Data Center Integrated Surface Database. In total, there are 1,614 weather stations across the continental United States with sufficient available data to run the ETRHEQ method. Because many of the stations are located in developed areas, such as on airport grounds, we adjust the weather station data to mitigate site-specific anomalies in temperature and dew point using data provided by Parameter Elevation Regression on Independent Slopes Model (PRISM; Daly et al., 2008). Specifically, we shift the weather station temperature and dew point measurements to match the monthly means of the PRISM data aggregated to 0.25° around the weather station (Rigden & Salvucci, 2015).

Precipitation data are from the Global Historical Climate Network Database (Menne et al., 2012). The occurrence of daily precipitation (but not amount) is an optional input to the ETRHEQ method used to temporally smooth estimates of C_{surf} , which otherwise fluctuate too much in response to synoptic weather variability.

Hourly net solar radiation values, which are also required by the ETRHEQ method, are from the Modern-Era Retrospective analysis for Research and Applications version 2 (MERRA-2) at 0.5° latitude by 0.625° longitude spatial resolution (GMAO, 2017). Weather stations are matched to the corresponding MERRA-2 grid box center that minimizes the distance between the station and grid center.

2.2.2. SM

Satellite-based near-surface SM estimates are from the SMAP Mission (Entekhabi et al., 2010). We utilize the SMAP Level-3 36-km radiometer product, which has a nominal return frequency of 3 days and an exact repeat frequency of 8 days. Note that these SM observations are not input to the ETRHEQ method but are used in the statistical model to partition ET into its source components.

2.2.3. LAI and Solar-Induced Fluorescence

LAI estimates are from the Moderate Resolution Imaging Spectroradiometer MOD15A2 product (C5), which is an 8-day composite at 500-m resolution from the Terra satellite (Knyazikhin et al., 1998; Yang et al., 2006). Solar-induced fluorescence (SIF) data are from the Global Ozone Monitoring Experiment-2 sensor onboard MetOp-A. We use the version 26 level 2 740-nm terrestrial chlorophyll fluorescence data set with 09:30 overpass local time (Joiner et al., 2013). All remotely sensed products are gridded onto the SMAP native 36-km EASE-2 grid using area-weighted averaging at daily scale. For station-level comparison, values from EASE-2 grid boxes with centers within 0.25° of the station are averaged, again at daily scale.

2.3. ET Partitioning Framework

Rather than estimating transpiration and soil evaporation from semiempirical vegetation and soil conductances, we decompose the estimated $C_{surf, EQ}$ into vegetation (C_{veg}) and soil (C_{soil}) conductances and use those to partition ET. This intermediate step of decomposing $C_{surf, EQ}$ is necessary because the ETRHEQ method is a diagnostic model and cannot be used in a way that allows soil and vegetation to respond separately to environmental perturbations.

When decomposing $C_{surf, EQ}$, we allow C_{veg} and C_{soil} to respond independently to environmental variables, such that

$$C_{surf} = f_v C_{veg}(S_d, VPD) + (1 - f_v) \times C_{soil}(S_d) \quad (1)$$

In equation (1), C_{veg} , C_{soil} , and the vegetation fraction (f_v) are estimated using an optimization model, which is described in detail below. We allow C_{veg} to vary with afternoon average vapor pressure deficit (VPD) and the degree of soil saturation (S_d ; defined as volumetric SM from SMAP divided by the porosity), that is, $C_{veg}(S_d, VPD)$, and C_{soil} to vary only with S_d , that is, $C_{soil}(S_d)$. VPD is calculated from meteorological measurements at the weather stations with afternoon defined as 12:30–4:30 PM local time. The f_v is allowed to vary spatially across 25 clusters, which are defined by clustering latitude and longitude using a k -means algorithm (Figure S2a). We tested additional clustering schemes with varying numbers of clusters and found the results to be qualitatively similar across tests. Ultimately, we use 25 clusters, as this number of clusters well captures the gradients in f_v while still allowing

Can easily find how they are accomplishing their main objective



Table 1

Summary Statistics Aggregated Across Land Cover Types and All Stations (Bottom Row), Including the Number of Stations in Each Land Cover Type (N); the Stomatal Slope Parameter (m); Vegetation Fraction (f_v); Vegetation and Soil Conductance (C_{veg} and C_{soil}); E/ET for Three SM Conditions, Including Dry, Intermediate (int), and Wet; and Average T/ET

Land cover type	N	m	f_v	C_{veg}	C_{soil}	$(\frac{E}{ET})_{dry}$	$(\frac{E}{ET})_{int}$	$(\frac{E}{ET})_{wet}$	$\frac{E}{ET}$
Evergreen needleleaf forest	36	0.49	0.31	8.2	1.48	0.24	0.28	0.3	0.7
Deciduous broadleaf forest	71	0.57	0.63	9.95	2.26	0.13	0.13	0.11	0.88
Mixed forest	142	0.54	0.64	9.42	2.28	0.14	0.14	0.12	0.87
Open shrublands	88	0.46	0.23	4.37	0.39	0.05	0.18	0.41	0.77
Woody savannas	211	0.50	0.57	7.47	2.09	0.18	0.2	0.17	0.82
Grasslands	429	0.45	0.46	6.55	0.91	0.05	0.11	0.21	0.87
Croplands	374	0.50	0.62	8.85	1.66	0.08	0.13	0.14	0.88
Cropland/natural vegetation	263	0.54	0.64	9.06	1.99	0.1	0.13	0.11	0.89
All stations	1,614	0.5	0.54	7.93	1.58	0.1	0.14	0.18	0.86

Note. All values are for the summertime.

the statistics within each cluster to converge. We do not fit f_v at each station to avoid overfitting the model, as each weather station only has 2 years of data.

Values of C_{veg} , C_{soil} , and f_v are estimated in an iterative process. First, a decision tree is used to partition the space defined by S_d and VPD into bins with at least 200 observations resulting in 646 partitions. In this initial partitioning, $C_{surf, EQ}$ is estimated assuming no bare soil evaporation (i.e., setting $f_v = 1$) and another decision tree is used to partition the space defined by S_d into nine partitions assuming no transpiration (i.e., setting $f_v = 0$). With these initial constraints, the model contains 680 unknowns, including 25 values of f_v (one for each cluster), 646 values of C_{veg} (which depend upon the partitions of S_d and VPD), and 9 values of C_{soil} (which depend upon the partitions of S_d).

We estimate these unknowns by fitting equation (1) to the over 400,000 daily values of $C_{surf, EQ}$ and maximizing the log likelihood. Because the conductance values are strictly positive, we base the likelihood on mean absolute deviations as opposed to sum-of-squares (Bloomfield & Steiger, 1983). Importantly, with guesses at the nine unknown values of C_{soil} in each SM partition and 25 values of f_v , the optimal value of C_{veg} in each of the 646 S_d -VPD partitions can be estimated from equation (1) as the median of $(C_{surf, EQ} - (1 - f_v)C_{soil})/f_v$. We use a genetic algorithm (MATLAB2017a, 2017) to fit the remaining 34 free parameters (f_v and C_{soil}) via maximum likelihood. The optimization is conducted efficiently with two a priori constraints: (1) values of C_{soil} and C_{veg} range between 0 and 15 mm/s, and (2) the predicted C_{surf} is positively correlated with f_v .

The estimation is run 10 times with different random initial guesses to ensure that a global optimum is reached. When the algorithm is run with synthetically generated data, it recovers all imposed functional forms of C_{veg} and C_{soil} , as well as the prescribed f_v (not shown). In the remaining text, we refer to the C_{surf} estimates from this decision tree framework as " $C_{surf, DT}$ ". Finally, the partitioning of ET can be estimated by assuming that $\frac{T}{ET} = \frac{f_v C_{veg}}{C_{surf, DT}}$.

The above ET partitioning method can be applied to data not derived from the ETRHEQ method. As seen in equation (1), the ET partitioning method requires daily C_{surf} , S_d , and VPD, and the source of these estimates does not change the approach (although, if C_{surf} is estimated from land surface parameterizations, the partitioning method would be circular and noninformative). We develop the ET partitioning method using ETRHEQ inferred C_{surf} because the ETRHEQ method has been shown to well capture C_{surf} inferred from measurements, and the ETRHEQ method allows C_{surf} to be estimated at an abundance of sites.

To summarize the ET partitioning results, we aggregate the model output from each weather station by geographical cluster, as well as by land cover type (Friedl et al., 2010; Table 1). Each weather station is assigned a land cover based on the dominant land cover type within a 0.25° box surrounding the station (Figure S2b).

Even though the paper is in a shorter "letter" format, enough information is provided to reproduce the results

The figure outlines methodology that does not rely heavily on the main text

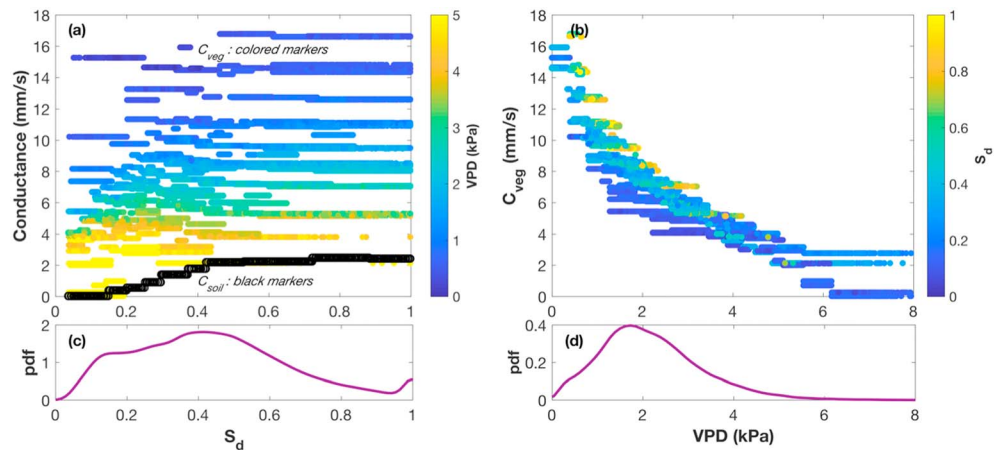


Figure 1. The C_{veg} and C_{surf} decision tree fit as a function of (a) soil saturation (S_d ; x-axis) and vapor pressure deficit (VPD; colors), (b) VPD (x-axis) and S_d (colors), and the probability density function (pdf) of summertime days with observed (c) S_d and (d) VPD (aggregated across all stations). Recall that C_{veg} is a function of S_d and VPD, and C_{soil} is a function of only S_d .

3. Results and Discussion

3.1. Model Fit

Overall, the optimization model fits the $C_{surf, EQ}$ estimates well with a daily root-mean-square error of 1.97 mm/s across all 1,614 stations. $C_{surf, DT}$ is slightly underestimated at high $C_{surf, EQ}$ values in the Appalachians and eastern Midwest (Figures S3a and S3b). Estimates of C_{veg} and C_{soil} are mapped in Figures S3c and S3d, and their dependence on environmental conditions are shown in Figure 1. When interpreting these results, it is important to recognize that the functional relationships in Figure 1 are not prescribed, and no information on greenness or vegetation fraction is input into the statistical decision tree model. The relationships in Figure 1 are estimated using only $C_{surf, EQ}$, remotely sensed SM, measured VPD, and the constraint implied by equation (1).

As shown in Figure 1a, both C_{veg} and C_{soil} increase with S_d and, for a given value of S_d , C_{veg} decreases with increasing VPD. Qualitatively, these relationships are both hydrologically and biologically consistent, as C_{soil} is expected to increase with SM, and stomatal conductance tends to increase when soils are relatively wet and the atmosphere is more humid. Additionally, the magnitude of C_{soil} is less than C_{veg} across the majority of S_d values, possibly reflecting that vegetation has access to deeper SM via roots and a large evaporative surface area (if $LAI \gg 1$).

As shown in Figure 1b, C_{veg} strongly declines as VPD increases. To quantitatively assess this dependence on VPD, we estimate the slope of the relationship between C_{veg} and VPD using a stomatal sensitivity model proposed by Oren et al. (1999), which takes the form: $g_s = 1 - m \ln(VPD)$, where g_s is the stomatal conductance and m is the slope. Using porometric and sap flow data, Oren et al. (1999) found that the value of m was approximately 0.6 across scales (from leaf to tree to stand), which is consistent with the theoretical value of m assuming stomata are regulating leaf potential near a constant value. Substituting g_s for C_{veg} , we estimate the value of m at approximately 0.5, ranging from 0.45 to 0.57 depending on land cover type (Table 1). The shallower slopes in grasslands ($m = 0.45$) and shrublands ($m = 0.46$) are consistent with both the wider range of VPD exhibited in water-limited conditions and the hypothesis that more drought tolerant species exhibit less strict regulation of leaf water potential at high VPD levels (Oren et al., 1999).

The relation between C_{veg} and VPD becomes increasingly important in the context of climate change, as VPD is predicted to increase over 50% by 2100 (Ficklin & Novick, 2017). Although declines in C_{veg} do not necessarily imply declines in transpiration, as increasing VPD still acts to increase evaporation from the stomatal pore, a strong enough stomatal response (i.e., a large m value) will reduce transpiration (Farquhar, 1978; Jones, 2014). For example, if we assume $T \sim VPD \times C_{veg} = VPD \times (1 - m \ln(VPD))$ and VPD ranges between 0 and 3 kPa, declines in T occur when m exceeds approximately 0.4, as shown in Figure S4. Unlike transpiration, an increase in VPD will always increase soil evaporation if water is available. This diverging response of

The main figure and its caption clearly explain the result of their approach, again not relying on main text

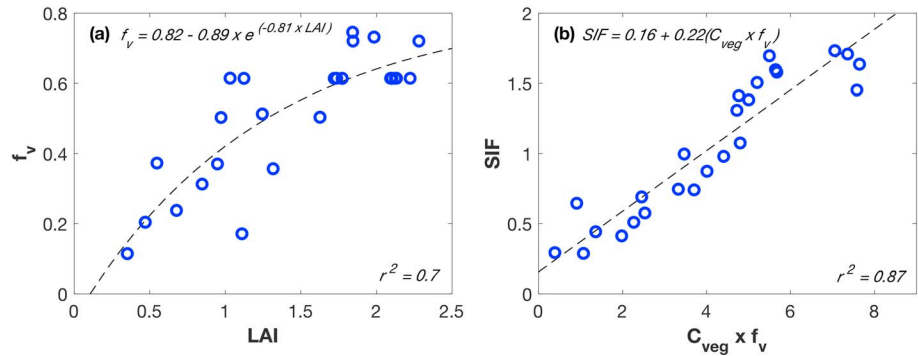


Figure 2. Comparison of (a) satellite-inferred LAI to modeled f_v and (b) modeled $C_{veg} \times f_v$ to observed SIF averaged over the two summers by geographic cluster (mapped in Figure S2a). In (a) the modeled variable (f_v) is on the y-axis to facilitate comparison with Figure 2a in Choudhury (1987). Fit equations and r^2 values are printed in each subplot. LAI = leaf area index; SIF = solar-induced fluorescence.

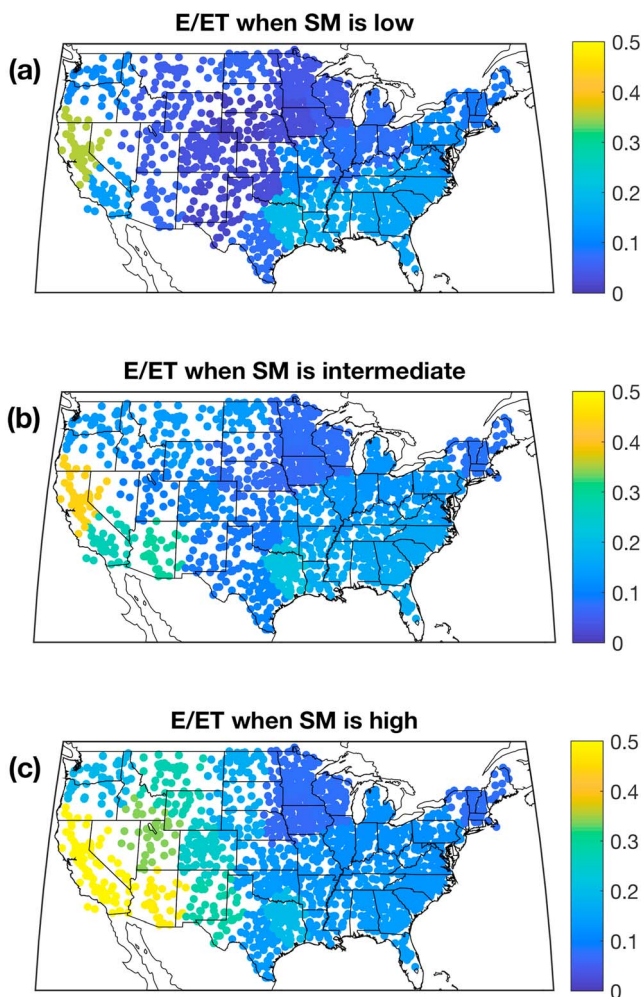


Figure 3. Fraction of soil evaporation contributing to total evaporation (E/ET) when (a) SM is low, (b) SM is intermediate, and (c) SM is high. The SM ranges are defined based on the quantiles for that station, as described in the text. SM = soil moisture; ET = evapotranspiration.

vegetation and soils to increases in VPD highlights the importance of accurately partitioning ET in Earth system models and is the topic of future work.

3.2. Comparison With LAI and SIF

To evaluate the model output, we compare estimates of modeled f_v to satellite-inferred LAI and modeled $f_v C_{veg}$ to satellite-observed SIF and find strong agreement between variables in both comparisons, as shown in Figure 2 and described below. In these comparisons, data are averaged spatially by cluster and temporally over both summers.

First, modeled f_v is positively correlated with satellite-inferred LAI ($r^2 = 0.70$), signifying that the model captures vegetation amount well across the 25 clusters. Rather than treating grid boxes as “mosaics” of vegetation and soil (as in this study), C_{veg} can also be modeled by scaling stomatal conductance by LAI (Stewart, 1988). Hence, f_v and LAI should be positively correlated as they both act to scale C_{veg} by vegetation amount. We identify an exponential relationship between f_v and LAI, consistent with observations (e.g., Choudhury, 1987).

Second, the estimated vegetation component of C_{surf} (i.e., $f_v C_{veg}$) is positively correlated with satellite-observed SIF ($r^2 = 0.87$). Recall that we are assuming that $\frac{T}{ET} = \frac{f_v C_{veg}}{C_{surf,DT}}$, which is equivalent to assuming that the $f_v C_{veg}$ term is proportional to transpiration. Thus, we are demonstrating a strong linear relationship ($r^2 = 0.87$) between SIF and T across the 25 clusters. A similar linear relationship between SIF and ET was recently demonstrated temporally for nonstressed conditions at an eddy covariance flux tower located in a temperate, mixed hardwood forest (Lu et al., 2018).

3.3. Assessing ET Partitioning

It is somewhat challenging to compare the ET partitioning estimates from this statistical model directly to field-scale observations because the lack of partitioning estimates specific to the summers of 2015 and 2016, and the large spatial and temporal variability in ET partitioning estimates between sites and years. Furthermore, recent synthesis analyses report annual ET partitioning averages (Schlesinger & Jasechko, 2014; Wang et al., 2014; Wei et al., 2017), while we focus exclusively on summertime fluxes. Presumably, since T/ET is positively related to LAI on average (Wang

et al., 2014; Wei et al., 2017), the summertime T/ET estimates presented in this study are larger than annual average T/ET. Consistent with previous findings though, our results suggest that transpiration dominates ET (Jasechko et al., 2013; Miralles et al., 2011; Schlesinger & Jasechko, 2014), particularly where LAI is high (Figure S5).

When aggregated by land cover type, we find that our results agree well with previous observational studies. Consistent with our results, Schlesinger and Jasechko (2014) found that observed T/ET in temperate deciduous forests is on average greater than T/ET in temperate coniferous forests, T/ET is on average lowest for shrublands, and T/ET in temperate grasslands is not significantly distinct from shrublands or forests. It is important to recognize that Schlesinger and Jasechko (2014) also demonstrated considerable overlap in T/ET across plant functional types and climates, highlighting the large variability in T/ET estimates.

To further assess the ET partitioning estimates, we separate the contribution of soil evaporation to total ET ($E/ET = 1 - T/ET$) in dry, intermediate, and wet conditions, as shown in Figure 3. For each station, we define “dry” conditions to be when the daily S_d is less than the 10th percentile, “intermediate” conditions to be when the daily S_d is between the 40th and 60th percentiles, and “wet” conditions to be when the daily S_d exceeds the 90th percentile. As shown in Figure 3 and Table 1, E/ET decreases from wet to dry conditions, specifically in the water-limited western United States. This signifies that, particularly in the western United States, the contribution of soil evaporation to ET decreases more rapidly with SM than the contribution of transpiration. This is expected, as plants have access to deeper soil reserves. Field studies have demonstrated that near-surface SM can decline below the wilting point with simultaneous increases in ET (e.g., Thompson et al., 2011), indicating that plants are accessing deeper moisture reserves via roots and modulating conductances accordingly. Dry spells can also lead to increased E/ET if water limitations stunt vegetation growth (e.g., Ferretti et al., 2003); however, identifying such temporal relationships is out of the scope of this study but a possible topic of future research.

4. Concluding Remarks

Accurately partitioning ET is one of the key research gaps in ET research (Fisher et al., 2017). Here we outline a methodology to estimate the partitioning of summertime ET using meteorological data and remotely sensed SM. We find a strong positive relationship between modeled f_v and satellite-inferred LAI, as well as between modeled $f_v C_{veg}$ and satellite-observed SIF, demonstrating that the method captures the spatial dynamics of vegetation activity during the summers of 2015 and 2016. Although recent research has focused on estimating ET from meteorological data (Gentine et al., 2016; Rigden & Salvucci, 2015), to our knowledge this is the first attempt to partition these ET estimates into vegetation and soil components.

Some limitations of this study include the following: (1) We do not take into account the evaporation of intercepted water from the canopy; (2) to estimate T/ET, we model the output of the ETRHEQ method, which not only facilitates this study but also increases uncertainty due to propagating errors; and (3) the model evaluation is limited, as comparable measurements of transpiration and bare soil evaporation are currently not available.

To constrain estimates of ET and the hydrologic cycle in future climates, it is critical we develop observation-based estimates of ET partitioning at large spatial scales. The sensitivity of ET to environmental factors depends on the sensitivity of each source component (Wang & Dickinson, 2012), and these sensitivities are not similar for transpiration and soil evaporation, as exemplified in the case of increasing VPD.

References

- Baldocchi, D. D., Vogel, C. A., & Hall, B. (1997). Seasonal variation of energy and water vapor exchange rates above and below a boreal jack pine forest canopy. *Journal of Geophysical Research*, 102(D24), 28,939–28,951. <https://doi.org/10.1029/96JD03325>
- Baldocchi, D. D., Xu, L., & Kiang, N. (2004). How plant functional-type, weather, seasonal drought, and soil physical properties alter water and energy fluxes of an oak-grass savanna and an annual grassland. *Agricultural and Forest Meteorology*, 123(1–2), 13–39. <https://doi.org/10.1016/j.agrformet.2003.11.006>
- Black, T. A., Gardner, W. R., & Thurtell, G. W. (1969). The prediction of evaporation, drainage, and soil water storage for a bare soil. *Soil Science Society of America Journal*, 33(5), 655–660. <https://doi.org/10.2136/sssaj1969.03615995003300050013x>
- Bloomfield, P., & Steiger, W. L. (1983). *Least absolute deviations: Theory, applications, and algorithms*. Boston, MA: Birkhäuser.
- Choudhury, B. J. (1987). Relationships between vegetation indices, radiation absorption, and net photosynthesis evaluated by a sensitivity analysis. *Remote Sensing of Environment*, 22(2), 209–233. [https://doi.org/10.1016/0034-4257\(87\)90059-9](https://doi.org/10.1016/0034-4257(87)90059-9)

The conclusion reads similarly to the abstract, but provides more detail

Main message and context are reiterated immediately



Acknowledgments

This material is based upon work supported by the National Science Foundation (NSF) under grant EAR-1446798. The meteorological data from NOAA's National Climatic Data Center Integrated Surface Database are available at <https://www.ncdc.noaa.gov/isd>. PRISM data are available at <http://www.prism.oregonstate.edu>. Precipitation data from the Global Historical Climate Network Database are available at <https://www.ncdc.noaa.gov/ghcn-d-data-access>. Solar radiation from Modern-Era Retrospective analysis for Research and Applications Version 2 (MERRA-2) are available at <https://disc.sci.gsfc.nasa.gov>. Soil moisture data from the Soil Moisture Active Passive (SMAP) satellite are available at <https://nsidc.org/data/smap/smap-data.html>. Funding for many of the AmeriFlux sites was provided by the U.S. Department of Energy's Office of Science, and data are available at <http://ameriflux.lbl.gov>. An example of the ETRHEQ method can be found at <https://github.com/AngelaRigden/ETRHEQ>.